

### 5.2.34 Effect of Li ion implantation on structural and optical properties of (K,Na)NbO<sub>3</sub> thin films

Radhe Shyam<sup>1</sup>, Deepak Negi<sup>1</sup>, Komal Shekhawat<sup>1</sup>, Fouran Singh<sup>2</sup>, Pargam Vashishtha<sup>3</sup>, Govind Gupta<sup>3</sup>, Subingya Pandey<sup>4</sup>, Pamu Dobbidi<sup>4</sup>, Srinivasa Rao Nelamarri<sup>1</sup>

<sup>1</sup>Department of Physics, Malaviya National Institute of Technology Jaipur, J.L.N. Marg, Jaipur 302017, India.

<sup>2</sup>Inter-University Accelerator Centre, Aruna Asaf Ali Marg, New Delhi 110067, India.

<sup>3</sup>CSIR-National Physical Laboratory, K.S. Krishnan Marg, New Delhi 110012, India.

<sup>4</sup>Department of Physics, Indian Institute of Technology Guwahati, Guwahati 781039, India.

KNN thin films were deposited on Si and quartz substrates at 250°C using RF magnetron sputtering under a pure Ar atmosphere. The sputtering was carried out at a power density of  $\sim 4.19$  W/cm<sup>2</sup>. The thickness of as-prepared samples was in the range of 350–400 nm. Subsequently, KNN films were annealed at 700°C for an hour to get the crystallinity of KNN perovskite. Thereafter, normal incident 30 keV Li ion implantation was done into crystalline KNN (pristine) thin films at fluences of  $3 \times 10^{14}$  ions/cm<sup>2</sup> (KNN-3E14),  $1 \times 10^{15}$  ions/cm<sup>2</sup> (KNN-1E15),  $3 \times 10^{15}$  ions/cm<sup>2</sup> (KNN-3E15),  $1 \times 10^{16}$  ions/cm<sup>2</sup> (KNN-1E16). The simulation of 30 keV Li ion into KNN matrix was performed using SRIM-2013 software. The electronic energy and nuclear energy losses are  $\sim 12$  eV/Å and 2.6 eV/Å, respectively. The projected range of 30 keV Li ion in the KNN matrix is  $\sim 138$  nm, which confirms that the Li ions are embedded in KNN thin films. The structural and optical properties of pristine and implanted KNN films were analyzed using different characterization techniques.

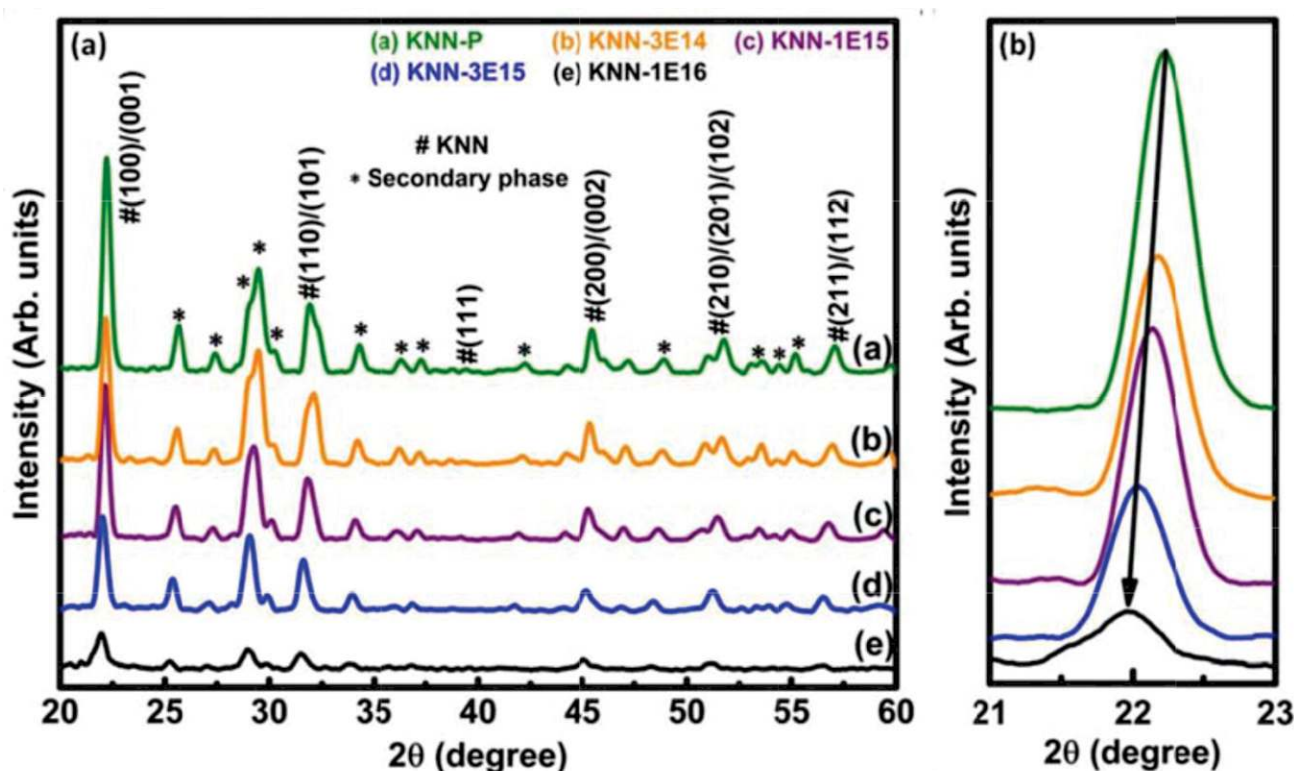


**Figure 1.** (a) XRD patterns of pristine and Li-ion implanted KNN thin films. (b) (001) peak shifting after ion implantation.

When the samples were subjected to Li ion implantation, the peak intensities of KNN perovskites get reduced with increase in ion fluence. Moreover, the continuous shifting of KNN related XRD peak towards the lower angle is observed with ion fluence, as shown in figure 1. The root-mean-square roughness ( $R_{\text{rms}}$ ) of pristine sample is  $\sim 13.7$  nm, which is reduced non-monotonously for implanted samples. The  $R_{\text{rms}}$  of implanted sample is in the range of 9.2–13.1 nm, where the KNN-3E14 sample exhibits a minimum roughness. A slight improvement in the optical transmittance of KNN films is noticed after ion implantation, but the variation is minimal. The optical band gap ( $E_g$ ) is nearly 3.62 eV for pristine KNN films, and a slight increasing behavior of  $E_g$  is found after ion implantation. The value of  $E_g$  is in range of 3.63–3.67 eV for the implanted samples. PL results indicate the improvement in near UV-Visible emission with similar PL characteristics as pristine KNN films, and the intensity increases exponentially with ion implantation fluence. TRPL shows the increase in decay lifetime after implantation

### 5.2.35 Engineering the properties of KNN thin films using 120 MeV Au ion beam irradiation

Radhe Shyam<sup>1</sup>, Deepak Negi<sup>1</sup>, Komal Shekhawat<sup>1</sup>, Fouran Singh<sup>2</sup>, Pargam Vashishtha<sup>3</sup>, Govind Gupta<sup>3</sup>, Subingya Pandey<sup>4</sup>, Pamu Dobbidi<sup>4</sup>, Srinivasa Rao Nelamarri<sup>1</sup>

<sup>1</sup>Department of Physics, Malaviya National Institute of Technology Jaipur, J.L.N. Marg, Jaipur 302017, India.

<sup>2</sup>Inter-University Accelerator Centre, Aruna Asaf Ali Marg, New Delhi 110067, India.

<sup>3</sup>CSIR-National Physical Laboratory, K.S. Krishnan Marg, New Delhi 110012, India.

<sup>4</sup>Department of Physics, Indian Institute of Technology Guwahati, Guwahati 781039, India.

KNN films were deposited on Si and quartz substrates using RF magnetron sputtering at a substrate temperature of 200°C. The deposition of KNN films was performed under pure argon ambience by maintaining a fixed sputtering power of 85 W. Afterwards, as-deposited samples were annealed in air ambience at 700°C for an hour to obtain crystalline KNN films (pristine films). Eventually, the crystalline KNN films were irradiated with 120 MeV Au ion beam at Inter-University Accelerator Centre (IUAC), New Delhi, India. Ion irradiation of KNN samples was done at various fluences such as  $5 \times 10^{11}$ ,  $1 \times 10^{12}$ ,  $5 \times 10^{12}$ , and  $1 \times 10^{13}$  ions/cm<sup>2</sup>, abbreviated as KNN-5E11, KNN-1E12, KNN-5E12, and KNN-1E13, respectively. The  $S_e$  and  $S_n$  values of 120 MeV Au ions in the KNN system are  $\sim 2.3$  keV/Å and 35.7 eV/Å, respectively, calculated using the SRIM-2013 simulation program. The projected Au ions (projected range  $\sim 10$  μm) go deep inside the substrate, and therefore, there is no possibility of Au ions getting embedded in the KNN matrix. The structural, morphological, chemical, and optical properties of ion irradiated films were studied using X-ray diffraction, scanning electron microscopy, UV-Vis spectroscopy, X-ray photoelectron spectroscopy, photoluminescence, and time-resolved PL spectroscopy.

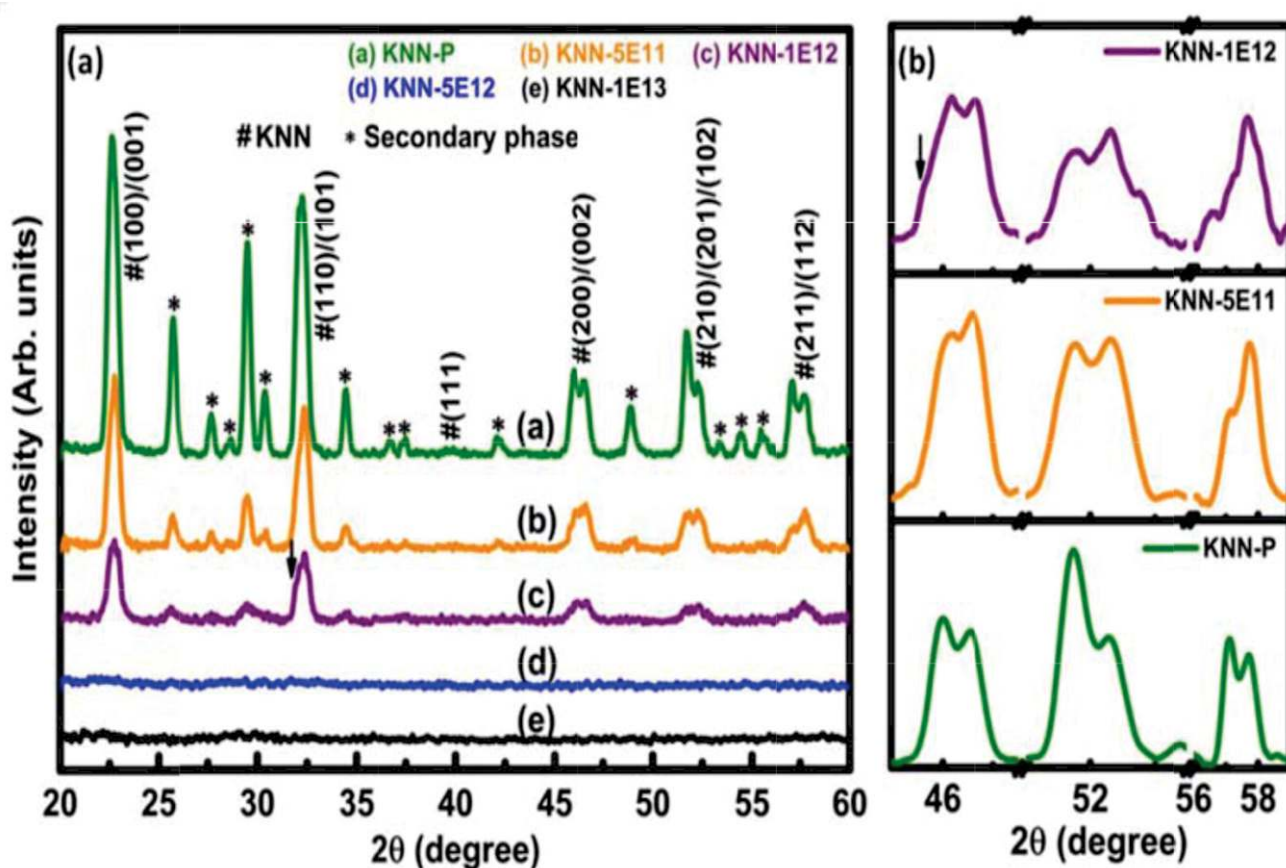


**Figure 1.** (a) XRD patterns of pristine and irradiated KNN samples. (b) Enlarged view of XRD pattern of pristine and KNN-5E11, KNN-1E12 samples.

After irradiation, the crystallinity of KNN perovskite is reduced with an increase in ion fluence, and the films get completely amorphized at higher fluences (Figure 1). The phase transitions are noticed with the increase in ion fluence. The surface morphology gets modified as an effect of irradiation, and a cluster of nano-sized grain-like microstructures are observed. XPS results indicate the loss of K content from the surface due to the volatile nature of alkali species. An improvement in transparency of KNN films is observed with ion fluence, and the optical band is found to increase with ion fluence. The PL intensity of irradiated KNN samples is enhanced with ion fluence, and the results are correlated to the grain size. TRPL results show the reduction of non-radiative recombination centers after ion beam irradiation.

### 5.2.36 Engineering of structural properties of $\text{Gd}_2\text{Zr}_2\text{O}_7$ via swift heavy ion irradiation

Asha Panghal<sup>1</sup>, Fouran Singh<sup>2</sup>, N. L. Singh<sup>1,3</sup>

<sup>1</sup>Department of Physics, The M. S. University of Baroda, Vadodara, 390002, India.

<sup>2</sup>Materials Science Group, Inter-University Accelerator Centre (IUAC), New Delhi -110067, India.

<sup>3</sup>Department of Physics, Netaji Subhas University of Technology, Delhi, 110078, India

Isometric pyrochlore oxides ( $\text{A}_2\text{B}_2\text{O}_7$ ) have prodigious structural and physical properties and are used in a variety of applications like electrolytes, sensors, immobilization of radioactive nuclides, and so on [1], [2]. Herein, the electronic excitation-induced disorder engineering in the  $\text{Gd}_2\text{Zr}_2\text{O}_7$  system on irradiation of 100 MeV  $\text{I}^{7+}$  ions with the function of fluence has been investigated. X-ray diffraction (XRD) and Raman spectroscopy techniques were performed for probe of electronic excitation-induced phase transformation. Rietveld refinement of the pristine  $\text{Gd}_2\text{Zr}_2\text{O}_7$  sample confirmed an ordered pyrochlore phase. XRD studies show that the superstructure reflection disappeared with the enhanced fluence, which indicates pyrochlore to defect fluorite structure phase transformation. Raman spectroscopy results demonstrate that the structural modifications of  $\text{Gd}_2\text{Zr}_2\text{O}_7$  samples depend strongly on the ion fluence and degrees of disorder augmented with enhanced ion fluence. Both, the complementary techniques provide the compatible elucidation of structural modifications induced by the swift heavy ions (100 MeV iodine) and demonstrate that no amorphization was observed in the  $\text{Gd}_2\text{Zr}_2\text{O}_7$  samples even after irradiation at the highest fluence and establish the capability of these samples as an actinide-bearing composition which can be applied as nuclear waste forms.

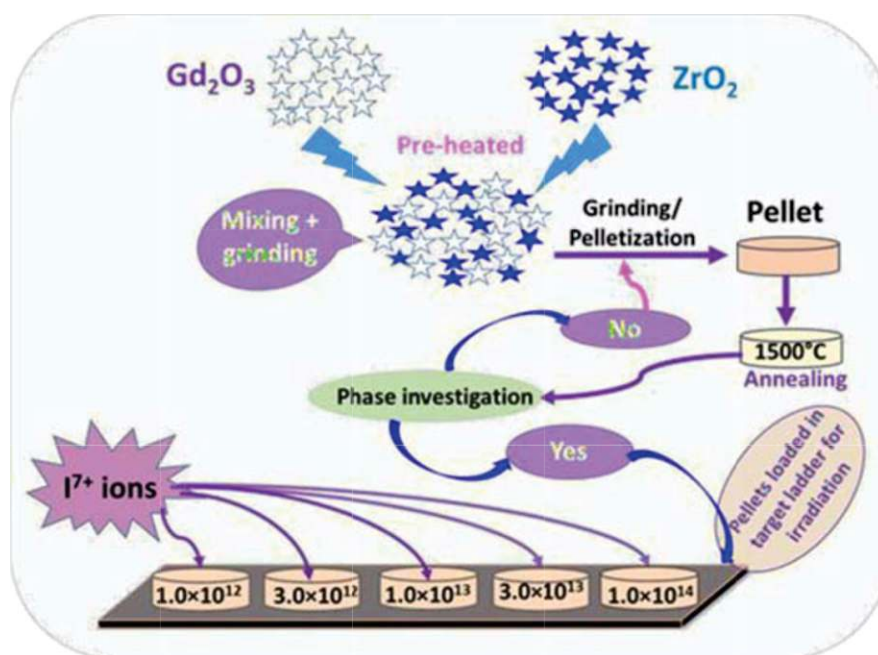


Fig. 1 shows the schematic diagram of experiment performed

Fig 1 shows the schematic diagram of experiment performed. The ion irradiation experiment was performed through 100 MeV  $\text{I}^{7+}$  (fluences,  $1.0 \times 10^{12}$  to  $1.0 \times 10^{14}$  ions/cm<sup>2</sup>) using 15 UD Pelletron accelerator facility at IUAC New Delhi. All irradiation experiments were performed at room temperature under the vacuum of  $10^{-6}$  mbar. The phase structure of  $\text{Gd}_2\text{Zr}_2\text{O}_7$  samples before and post irradiated was investigated using the Bruker D8 Advance diffractometer (Cu K $\alpha$  radiation,  $\lambda = 1.5406 \text{ \AA}$ ) with a step size of  $0.02^\circ$  in the range of  $10^\circ$ - $75^\circ$ . Surface morphology and microstructure of pristine  $\text{Gd}_2\text{Zr}_2\text{O}_7$  were examined employing Field emission scanning electron microscopy (FE-SEM, Supra 55 Zeiss). A thin layer of gold has been coated on the pristine  $\text{Gd}_2\text{Zr}_2\text{O}_7$  sample to nullify the charging phenomenon. The Raman spectra of pre and post irradiated samples within the range of  $100 \text{ cm}^{-1}$  to  $800 \text{ cm}^{-1}$  was recorded using the Jobin-Yvon Horiba LABRAM-HR dispersive spectrometer. The electronic energy loss ( $S_e$ ) and nuclear energy loss ( $S_n$ ) were calculated using the SRIM-2013 [3]. The value of  $S_n$  and  $S_e$  suggest that energy in the  $\text{Gd}_2\text{Zr}_2\text{O}_7$  composition is significantly deposited by the electronic excitation processes. Fig. 2 (a) represents the XRD pattern, (b) represents the Williamson-Hall plot, and (c) represents the Rietveld refinement of pristine  $\text{Gd}_2\text{Zr}_2\text{O}_7$ . The crystallite size and lattice strain were deduced from Williamson-Hall (W-H) plot [4,5] as displayed in Fig. 2 (b). To get more insight into the crystal structure and unit cell parameter, Rietveld refinement was executed on the diffraction patterns of pristine  $\text{Gd}_2\text{Zr}_2\text{O}_7$  sample using the Fullprof program [6]. Fig. 2 (c) displays the Rietveld refinement of the pristine  $\text{Gd}_2\text{Zr}_2\text{O}_7$  sample. The pseudo-Voigt function was utilized to refine the experimental data. In the refined XRD pattern, the black color line represents the experimental (observed) data and the red color line depicts the refined (calculated) data. The bottom blue line signifies the difference between the observed and refined data. The vertical magenta line exhibits the Bragg positions. (The superstructure reflections are



marked with an asterisk '\*'). The Rietveld refinement of the pristine  $\text{Gd}_2\text{Zr}_2\text{O}_7$  sample confirmed that the  $\text{Gd}_2\text{Zr}_2\text{O}_7$  has ordered pyrochlore structure as a major phase. X-ray diffraction results show that the irradiation-induced structural modifications, i.e., pyrochlore to the fluorite phase transition of  $\text{Gd}_2\text{Zr}_2\text{O}_7$  ceramics are strongly ion fluence dependent. The  $\text{Gd}_2\text{Zr}_2\text{O}_7$  samples irradiated for initial fluences ( $1.0 \times 10^{12}$  ions/cm<sup>2</sup> and  $3.0 \times 10^{12}$  ions/cm<sup>2</sup>) present the least degree of phase fraction. The Raman spectroscopy studies revealed the formation of the pyrochlore phase with weak subtle pyrochlore ordering. The present study reveals that the  $\text{Gd}_2\text{Zr}_2\text{O}_7$  system did not show evidence of radiation-induced amorphization, even for high electronic energy loss. The study of effect on simple oxides upon irradiation with 120 MeV Ag and 80 MeV Si are being characterized via different characterization technique and analysis is under process.

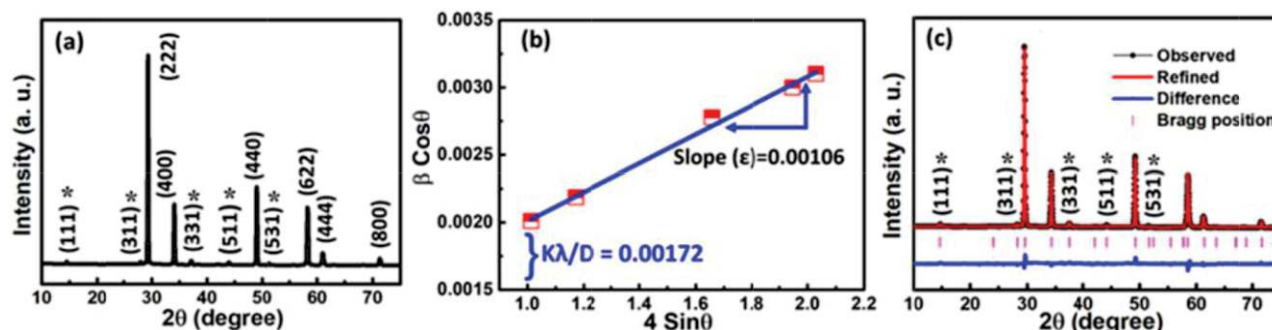


Fig. 2 (a) represents XRD pattern, (b) Williamson-Hall plot, and (c) Rietveld refinement of pristine  $\text{Gd}_2\text{Zr}_2\text{O}_7$ . (The superstructure reflections are marked with an asterisk '\*').

## REFERENCES:

- [1] K. Liu, K. Zhang, T. Deng, J. Zeng, B. Luo, H. Zhang, *Ceram. Int.* 1-11(2021)
- [2] M. Jafar, S.B. Phapale, B.P. Mandal, M. Roy, S.N. Achary, R. Mishra, A.K. Tyagi, *J. Alloys Compd.* **867**, 159032 (2021).
- [3] A. Panghal, Y. Kumar, P.K. Kulriya, P.M. Shirage, N.L. Singh, *J. Alloys Compd.* **862**, 158556 (2021).
- [4] G. Williamson, W. Hall, X-ray line broadening from filed aluminium and wolfram, *Acta Metall.* **1**, 22-31(1953).
- [5] Y. Kumar, A.K. Rana, P. Bhojane, M. Pusty, V. Bagwe, S. Sen, P.M. Shirage, *Mater. Res. Express.* **2**, 105017(2015).
- [6] S.X. Wang, B.D. Begg, L.M. Wang, R.C. Ewing, W.J. Weber, K. V. Govidan Kutty, *J. Mater. Res.* **14**, 4470-4473(1999).

### 5.2.37 Semiconductor-to-metal transition in nanocomposites of wide bandgap oxide semiconductors

Himanshi Gupta<sup>1</sup>, Naina Gautam<sup>2</sup>, Subodh K Gautam<sup>1,3</sup>, R.G. Singh<sup>4</sup>, and Fouran Singh<sup>1,\*</sup>

<sup>1</sup>Materials Science Group, Inter-University Accelerator Centre, Aruna Asaf Ali Marg, New Delhi-110067, India

<sup>2</sup>Department of Electronic Science, University of Delhi South Campus, New Delhi - 110023, India

<sup>3</sup>Laboratory of Solid-State Physics (LPS), University of Paris-Sud, 91400 Orsay, France

<sup>4</sup>Department of Physics, Bhagini Nivedita College, University of Delhi, New Delhi-110043, India

The Zinc oxide (ZnO) possesses unique properties like as a wide bandgap of 3.37 eV and a large exciton binding energy of 60 meV; due to these properties, it is a potential candidate for many applications from LED to solar cells [1]. On the other hand, the cadmium oxide (CdO) has a band of 2.2 eV, due to which it possesses high transparency in the visible region and low resistive nature. Thus, mixing CdO with ZnO can prove a good candidate for device applications such as optoelectronics. To utilize the ZnO/CdO nanocomposites thin films for device applications it is important to understand the electrical charge transport mechanisms of these films at low temperatures. It was that Gadoped ZnO thin films exhibit the peculiar phenomenon of semiconductor-to-metal transition (SMT) with increasing Ga concentration reported by V. Bhosle et al. [2] and was explained within the weak-localization model framework and variable range hopping (VRH) mechanism [3,4]. In the case of a higher degree of disorder, the charge transport could not be explained with classical models alone; one needed to incorporate quantum effects [5,6]. Whereas observation of SMT in polycrystalline ZnO thin films by creating controlled defects via ion irradiations was reported by Fouran Singh et al. [7]. Most studies have been explained well by incorporating quantum correction to conductivity (QCC) term to the well-known Boltzmann conductivity relation. The weak localization effect and renormalized electron-electron interaction are the two factors responsible for quantum correction to the conductivity [6]. In this study SMT is reported in nano composite films of wide bandgap semiconducting oxides and it offers an insight into the existing models of temperature-dependent charge transport by tailoring the defects induced disorder into the lattice by SHIs irradiation. Temperature-dependent charge transport properties of the films were studied by carrying out four-probe resistivity measurements in the wide temperature range of 40–300 K. It is observed that SHIs can be used to tune the SMT behaviour and its transition temperature upon increasing fluence of irradiation. These irradiation effects are discussed in terms of irradiation-



induced defects/disorders into the lattice. The change in temperature-dependent resistivity in films has been envisaged with a quantitative fit of experimental data by invoking QCC. The results agree with this model, which essentially depends on weak localization and renormalized electron-electron interactions. Thus, this work extends the validity of the weak localization model to composite systems. [For details see *Journal of Alloys and Compounds* 894 (2022) 162392]

#### REFERENCES:

- 1) Ü. Özgür, *et.al.* A comprehensive review of ZnO materials and devices, *J. Appl. Phys.* **98**, 041301(2005).
- 2) V. Bhosle, A. Tiwari, J. Narayan, Electrical properties of transparent and conducting Ga doped ZnO, *J. Appl. Phys.* **100**, 033713(2006).
- 3) Y. Li, Q. Huang, X. Bi, The change of electrical transport characterizations in Ga doped ZnO films with various thicknesses, *J. Appl. Phys.* **113**, 053702(2013).
- 4) M. Sbata, T. Serin, A. Yildiz, Determination of the critical carrier concentration for the metal–insulator transition in Ga-doped ZnO, *J. Mater. Sci. Mater. Electron.* **29**, 14111–14115 (2018).
- 5) Y.J. Zeng, *et.al.* Tuning Quantum Corrections and Magnetoresistance in ZnO Nanowires by Ion Implantation, *Nano Lett.* **12**, 666–672(2012).
- 6) A.K. Das, R.S. Ajimsha, L.M. Kukreja, Quantum corrections to temperature dependent electrical conductivity of ZnO thin films degenerately doped with Si, *Appl. Phys. Lett.* **104**, 042112(2014).
- 7) Fouran Singh, *et.al.* Disorder induced semiconductor to metal transition and modifications of grain boundaries in nanocrystalline zinc oxide thin film, *J. Appl. Phys.* **112**, 073101(2012).

#### 5.2.38 Gamma-ray induced modifications on ZrO<sub>2</sub> thin films: structural and optical properties

Vishnu Chauhan<sup>a,b</sup>, and Rajesh Kumar<sup>b</sup>

<sup>a</sup>Materials Science Group, Inter-University Accelerator Centre, Aruna Asaf Ali Marg, New Delhi, 110067, India

<sup>b</sup>University School of Basic and Applied Sciences, Guru Gobind Singh Indraprastha University, New Delhi, 110078, India

The structural and optical properties of RF sputtering deposited zirconium oxide (ZrO<sub>2</sub>) thin films have been modified using high dose gamma irradiation at Inter-University Accelerator Center (IUAC), New Delhi. ZrO<sub>2</sub> thin films have been irradiated for different doses from 500 kGy to 2000 kGy. After gamma exposure, ZrO<sub>2</sub> thin films have sustained their monoclinic and tetragonal structure, but the intensity and position of the planes is found to be varied significantly. On the account of gamma irradiation, it may be inferred that the release of photon energy results into decrease in crystallite size and shifting of the XRD peaks occurred which can be ascribed to release of residual stress from the films. UV-Vis study remarked that the optical band gap showed a red-shifting in the absorption edges in gamma irradiated samples as compared to their pristine counterparts. This signifies the decrease in values of band gap (4.29 – 3.59 eV) after gamma exposure of ZrO<sub>2</sub> thin films. The empirical relation has been used to determine the Urbach energy that depicts the band-tail *i.e.*  $\ln(\alpha) = \ln(\alpha_0) + \ln(h\nu/E_u)$ . In PL study, mainly ZrO<sub>2</sub> films showed two emission bands at 423 nm and 532 nm. The observed bands have been deconvoluted for better understanding of the PL emission processes. The emission band appeared at 483 nm corresponds to blue emission and 520 nm corresponds to intrinsic defects related to oxygen vacancies. A clear noticeable change has been observed in shape, intensity and FWHM of PL emission peaks of high dose gamma exposed thin films. The study investigates that the changes observed in PL emission peaks in ZrO<sub>2</sub> samples might be due to formation of oxygen vacancies and surface defects. The structural and optical study also suggests the possibility of using ZrO<sub>2</sub> thin films for  $\gamma$ -dosimetry applications at high doses. [for details, see *optical materials* 126 (2022) 112125]1.

#### REFERENCES:

- [1]. V. Chauhan *et al.* Influence of high dose gamma radiation on optical, physico-chemical and surface morphology properties of nanocrystalline ZrO<sub>2</sub> thin films, *Optical Materials* **126**, 112125(2022).

#### 5.2.39 Signature of strong localization and crossover conduction processes in doped zno thin films: synergetic effect of doping fraction and dense electronic excitations

Himanshi Gupta<sup>1</sup>, Jitendra Singh<sup>1,2</sup>, G.R. Umapathy<sup>1</sup>, Vijay Soni<sup>1</sup>, S. Ojha<sup>1</sup>, Soumen Kar<sup>1</sup>, and Fouran Singh<sup>1\*</sup>

<sup>1</sup>Inter-University Accelerator Centre, New Delhi -110067, India.

<sup>2</sup>National Taiwan University of Science and Technology, Taipei-Taiwan.

Ga<sub>x</sub>Zn<sub>1-x</sub>O thin films (x = 1 at.%, 3 at.%, and 5 at.%) of thickness 280 nm were deposited on a corning glass and silicon substrates using the sol-gel spin coating method, and detailed synthesis procedure reported elsewhere[1]. The as-deposited films were annealed in an oxygen environment at 500°C using a GERO tubular furnace. One film

of each composition was kept as a reference (pristine), and other films were irradiated with 120 MeV  $\text{Ag}^{+9}$  ions using a 15UD Tandem Pelletron accelerator at IUAC, New Delhi. The films were irradiated for the ion fluences of  $3 \times 10^{13}$  ions/cm<sup>2</sup> and  $5 \times 10^{13}$  ions/cm<sup>2</sup>. After that the influence of Ga-doping and high energy ion irradiation on the structural, optical, and electrical charge transport properties was studied using various characterization techniques such as X-Ray Diffraction, scanning electron microscopy, UV-Vis spectroscopy, and temperature dependent resistivity through homemade set-up named as variable temperature insert cryogen-free magnet system (VTI- CFMS). From the XRD pattern it is found that the films remain crystalline even at higher doping fraction and irradiation with high ion fluence. The transmission spectra reveal that the films exhibit good transmittance in the visible region and a reduction of about 20% in transmittance was observed for irradiated films at higher ion fluences. The Urbach energy was estimated and showed an augmenting response upon increase in doping fraction and ion irradiation, this divulges an enhancement of localized states in the bandgap or disorder in the films. The evolution of such localized states plays a vital role in charge transport and thus the temperature dependent electrical conductivity of irradiated thin films was studied to elucidate the dominant conduction mechanisms. The detailed analysis unfolds that in the high-temperature regime ( $180\text{K} < T < 300\text{K}$ ), the charge conduction was dominated by thermally activated band conduction followed by the nearest neighbor hopping (NNH) mechanism. Whereas in the lower temperature regime ( $25\text{K} < T < 170\text{K}$ ), the conduction mechanism was governed by Mott-VRH (variable range hopping) followed by Efros-Shklovskii (ES)-VRH. A sudden and steep rise in resistivity below 30K was observed for GZO films with higher doping fraction at higher ion fluence and proclaims the presence of strong localization of carriers. [See details in *Journal of Physics: Condensed Matter* 30, 315701 (2021)].

## REFERENCES:

- [1] H. Gupta *et al.*, “Defect-induced photoluminescence from gallium-doped zinc oxide thin films: influence of doping and energetic ion irradiation,” *Phys. Chem. Chem. Phys.*, vol. **21**, no. 27, pp. 15019–15029 (2019), doi: 10.1039/C9CP02148E.

### 5.2.40 Tuning of visible photo luminescence by defects induced by swift heavy ion irradiation in zinc oxide films

R.G. Singh<sup>1</sup>, Himanshi Gupta<sup>2</sup>, R. M. Mehra<sup>3</sup>, and Fouran Singh<sup>2,\*</sup>

<sup>1</sup>Department of Physics, Bhagini Nivedita College, University of Delhi, New Delhi -110043, India.

<sup>2</sup>Inter-University Accelerator Centre, New Delhi -110067, India.

<sup>3</sup>School of Electronics and Communication Engineering, Sharda University, Greater Noida (U.P.)- 201308, India

The as-deposited ZnO thin films were thermally annealed in two different environments (oxygen and argon) at two different annealing temperatures (500 °C and 700 °C) for 1 hour. Further, all the thin films were irradiated with 50 MeV Ni and 120 MeV Au ions at varying ion fluences using 15 UD tandem accelerator at IUAC, New Delhi, India. All films were irradiated for ion fluence of  $5 \times 10^{10}$  ions/cm<sup>2</sup>,  $3 \times 10^{11}$  ions/cm<sup>2</sup>,  $1 \times 10^{12}$  ions/cm<sup>2</sup>,  $3 \times 10^{12}$  ions/cm<sup>2</sup>, and  $1 \times 10^{13}$  ions/cm<sup>2</sup>. Before and after irradiation ZnO films were characterized by GAXRD, AFM, and photoluminescence spectroscopy (PL) techniques. The microstructure of the films was modified by the controlled thermal annealing and the nature of defects are tuned by swift heavy ions (SHI) irradiations at varying ion fluences of such thin films. It is observed that all the films show two emission bands in the spectral range of 350 nm to 1000 nm; (i) a very weak UV- emission band and (ii) a broad visible emission band. The UV-emission band is attributed to the band to band transition while the visible emission to the deep-level defects. The maximum visible emission lies in the green emission region which enhanced with increasing annealing temperature for the samples annealed Ar-environment in comparison of samples annealed in an oxygen environment. The intensity of the visible emission band was also increased with ion irradiation at low ion fluences while showing reduction at higher ion fluences along with peak broadening. The films annealed at higher annealing temperature exhibit shifting of peak maximum from green region to red region at higher fluences. The peak shifting and peak broadening at higher ion fluences could be attributed to the formation of the high density of complex defects such vacancies cluster and ionized oxygen vacancies in the lattice as tuned under the influence of electronic energy deposition through SHI irradiations[1]. Thus, it is reported that the intense luminescence induced by the defects could be tuned in controlled manner by selecting the proper irradiations parameters and thus it would be very interesting for the development of the optoelectronic applications. (For details see *Radiation Physics and Chemistry* **183** (2021), 109400)

## REFERENCES:

- [1] R. G. Singh, H. Gupta, R. M. Mehra, and F. Singh, “Tuning of defects induced visible photoluminescence by swift heavy ion irradiation and thermal annealing in zinc oxide films,” *Radiat. Phys. Chem.*, vol. **183**, no. February, p. 109400, Jun(2021), doi: 10.1016/j.radphyschem.2021.109400.

### 5.2.41 Investigation of structural, morphological, and optical properties of $\text{MgTiO}_3$ thin films using high energy ion beam irradiation

Deepak Negi<sup>1</sup>, Radhe Shyam<sup>1</sup>, Komal Shekhawat<sup>1</sup>, Pargam Vasistha<sup>2</sup>, Govind Gupta<sup>2</sup>, Fouran Singh<sup>3</sup>, Srinivasa Rao Nelamarri<sup>1</sup>

<sup>1</sup>Department of Physics, Malaviya National Institute of Technology Jaipur, J. L. N. Marg, Jaipur-302017, Rajasthan, India.

<sup>2</sup>CSIR-National Physical Laboratory, K. S. Krishnan Marg, New Delhi, 110012, India.

<sup>3</sup>Materials Science Group, Inter-University Accelerator Centre, Aruna Asaf Ali Marg, New Delhi-110067, India.

The effects of high energy ion beam irradiation on structural, morphological, and optical properties of RF sputtered  $\text{MgTiO}_3$  (MTO) thin films were studied. The films were deposited on Si and quartz substrates using RF magnetron sputtering in pure Ar atmosphere. Subsequently, the films were annealed at 750°C for crystallization. Afterward, the films were irradiated using Swift Heavy Ions (SHI) of  $\text{Si}^{6+}$  and  $\text{Au}^{9+}$  with energy 80 MeV and 120 MeV, respectively. The irradiation was carried out at fluences of  $1 \times 10^{12}$ ,  $5 \times 10^{12}$  and  $1 \times 10^{13}$  ions/cm<sup>2</sup> using 15 UD Pelletron tandem accelerator at Inter-University Accelerator Centre (IUAC), New Delhi. Subsequently, the pristine (annealed at 750°C) and irradiated samples were characterized using X-ray diffraction, atomic force microscopy, and UV-Vis-NIR spectroscopy at MNIT Jaipur. The luminescent properties and decay lifetime of pristine and irradiated films were investigated using photoluminescence (PL) spectroscopy and time-resolved PL at CSIR- National Physical Laboratory (NPL), New Delhi.

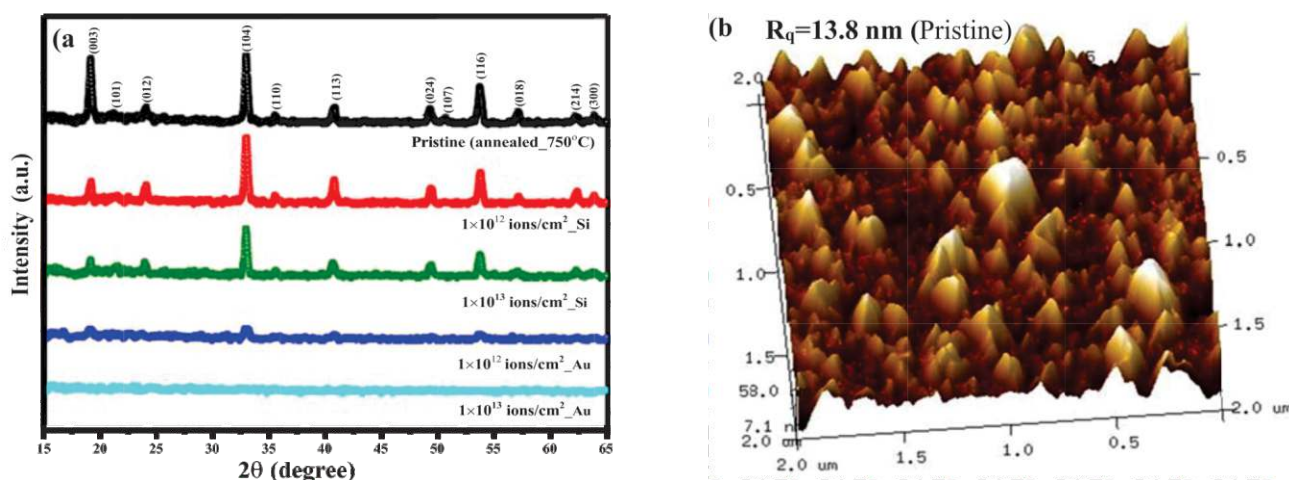


Fig 1. (a) XRD pattern of pristine and irradiated MTO thin films at different fluences using Si and Au ions, (b) AFM image of pristine MTO thin film

Well defined peaks as evident from XRD pattern, shown in fig 1 (a), confirm the rhombohedral crystal structure with (104) preferred orientation. The crystallinity is observed to decrease upon irradiation with increase in fluence from  $1 \times 10^{12}$  to  $1 \times 10^{13}$  ions/cm<sup>2</sup> in case of Si irradiated films. Also, the crystallinity drastically decreases with Au ion irradiation, while the films get completely amorphized at fluence of  $1 \times 10^{13}$  ions/cm<sup>2</sup>. The pristine MTO film possesses rms roughness ( $R_q$ ) of 13.8 nm (shown in fig 1 (b)), which is observed to decrease upon ion beam irradiation. The films irradiated with Au ions exhibit more roughness with agglomerated grains as compared to the Si irradiated films. The optical bandgap of pristine MTO film is 4.26 eV, which is narrowed down to 4.16 eV after ion beam irradiation with Si ions at a fluence of  $1 \times 10^{12}$  ions/cm<sup>2</sup>, which is further decreased to 4.10 eV upon increasing the fluence to  $1 \times 10^{13}$  ions/cm<sup>2</sup>. For the films irradiated with Au ions, the bandgap is reduced from 3.94 to 3.76 eV with increasing the fluence from  $1 \times 10^{12}$  to  $1 \times 10^{13}$  ions/cm<sup>2</sup>. The pristine films show intense PL emission in the UV region as well as weak peaks in the visible region. Peak broadening and decrease in PL intensity was observed after irradiation. The reduction in PL intensity is more significant in case of Si ion irradiation. The decay lifetime of photogenerated charge carriers for pristine and irradiated samples is in the order of a few nanoseconds.

### 5.2.42 Effects of 120 MeV $\text{Ag}^{9+}$ SHI irradiation on the structural, optical and electrical properties of pristine and Ni doped $\text{BiFeO}_3$ thin films grown by pulsed laser deposition

M. Nadeem<sup>1</sup>, Wasi Khan<sup>2</sup>, Shakeel Khan<sup>1</sup>, Fouran Singh<sup>3</sup>, R.J. Choudhary<sup>4</sup>, D.K. Shukla<sup>4</sup>, Sumesh Rana<sup>4</sup>, R. Venkatesh<sup>4</sup> and S.R. Sahu<sup>4</sup>

<sup>1</sup>Department of Applied Physics, Z.H. College of Engineering & Technology, Aligarh Muslim University, Aligarh-202002, India

<sup>2</sup>Department of Physics, Aligarh Muslim University, Aligarh-202002, India

<sup>3</sup>Inter-University Accelerator Centre, Aruna Asaf Ali Marg, New Delhi-110067, India

<sup>4</sup>UGC-DAE Consortium for Scientific Research, Khandwa Road, Indore-452017, India